Synthesis and characterization of Thio/Seleno-Urea/ Semicarbazone derivatives for Anti-Alzheimer studies

IISER PUNE

Thesis submitted in partial fulfilment of the requirements of the BS-MS Dual Degree Program at IISER, Pune.

Submitted by

Harini.P

20171074

Under the guidance of

Dr. R. Karvembu

Department of Chemistry, NIT-Trichy.

Certificate

This is to certify that this dissertation entitled "**Synthesis and characterization of Thio/seleno-urea/semicarbazone derivatives for Anti-Alzheimer studies**" towards the partial fulfilment of the BS-MS dual degree programme at the Indian Institute of Science Education and Research, Pune represents study/work carried out by Harini.P at the National Institute of Technology-Trichy under the supervision of Dr.R.Karvembu**,** Associate Professor, Department of Chemistry during the academic year Jan-Dec 2022.

Harini.P,

BS-MS,

IISER-Pune.

Dr.R.Karvembu,

Associate Professor,

NIT-Trichy.

DECLARATION

I hereby declare that the matter embodied in the report entitled "**Synthesis and characterization of Thio/seleno-urea/semicarbazone derivatives for Anti-Alzheimer studies**" are the results of the work carried out by me at the Department of Chemistry, National Institute of Technology-Trichy, under the supervision of Dr.R.Karvembu and the same has not been submitted elsewhere for any other degree.

Harini.P,

BS-MS,

IISER-Pune.

Dr.R.Karvembu,

Associate Professor,

NIT-Trichy.

ACKNOWLEDGEMENT

CONTENTS

1. Abbreviations

NMR	Nuclear Magnetic Resonance
HRMS	High-Resolution Mass Spectrometry
FT-IR	Fourier Transform- Infrared Spectroscopy
J	Coupling Constant
Hz	Hertz
MHz	Megahertz
EtOAc	Ethyl Acetate
DCM	Dichloromethane
TLC	Thin Layer Chromatography
TSC	Thiosemicarbazone
UV	Ultraviolet-visible spectroscopy
DMSO	Dimethyl Sulfoxide
TSC	Thiosemicarbazone

2. List of Figures

3. List of tables

4. List of schemes

5. Abstract

Thioureas/Thiosemicarbazones are small molecules studied extensively in drug design due to their wide range of biological activities. Selenium is shown to be involved in various metabolic processes in the human body, and low Se levels are observed in the plasma regions of AD patients. Based on this fact, we have synthesized Thiosemicarbazone ligands and Acyl-selenourea ligands as inhibitors of Aβ aggregation. We hypothesize that the seleno-derivatives will exhibit higher activity than their thio-derivatives. We have also conducted in-silico studies to gain a broader view of the interactions which take place. The docking studies show that there is no considerable difference in the binding abilities and the interactions of the synthesized Acyl-selenourea ligands compared to their corresponding acyl-thiourea counterparts.

6. Introduction

6.1 Alzheimer's disease (AD)

AD is one of the most prevalent neurodegenerative disease, characterized by a progressive and irreversible decline in cognitive functions, that constitutes around 55-60% of dementia patients worldwide. Currently, the estimation of people affected by AD is around 47 million people, and World Health Organisation (WHO) has estimated that by 2050, this number will multiply to 150 million. Alzheimer's disease was officially listed as the sixth leading cause of death in the United States in 2019 and the seventh-leading cause of death in 2020 and 2021, when COVID-19 entered the ranks of the top ten causes of death [1]. The total cost of AD is expected to surpass 1 trillion dollars annually, and it is also known that AD causes enormous mental stress on caretakers.

Until recently, there were no clinically approved drugs for AD that directly affected the disease's progression, and the FDA-approved drugs only worked on providing symptomatic relief. The four approved drugs are donepezil, galantamine, rivastigmine which acts as an AChE inhibitor, and memantine which is an N-methyl-D-aspartate antagonist. In 2021, a new drug named Aducanumab was approved by FDA for the treatment of AD through the accelerated approval program amid controversial results. Aducanumab is a monoclonal antibody that shows selective binding to misfolded amyloid-beta oligomers, which causes a reduction in the amount of amyloid-beta plaques in the brain. But the above has not been shown to have any effect on memory and cognitive abilities.

6.2 Amyloid Hypothesis

While the complex neuropathology of AD is not known completely, the most extensively approved theory is the Amyloid hypothesis (Figure1), according to which the first component of AD is characterized by an increase in the level of aggregated amyloid-beta peptide in the brain, which is then followed by tau-protein hyperphosphorylation and another cascade of events(including changes in the levels of multiple prominent neurotransmitters such as Acetylcholine, Butylcholine, Serotonin,

Dopamine, Norepinephrine, and several Monoxidases), eventually ending in neuronal degeneration and apoptosis [2]. In the amyloid hypothesis, Amyloid precursor protein (APP) becomes the starting point of AD.
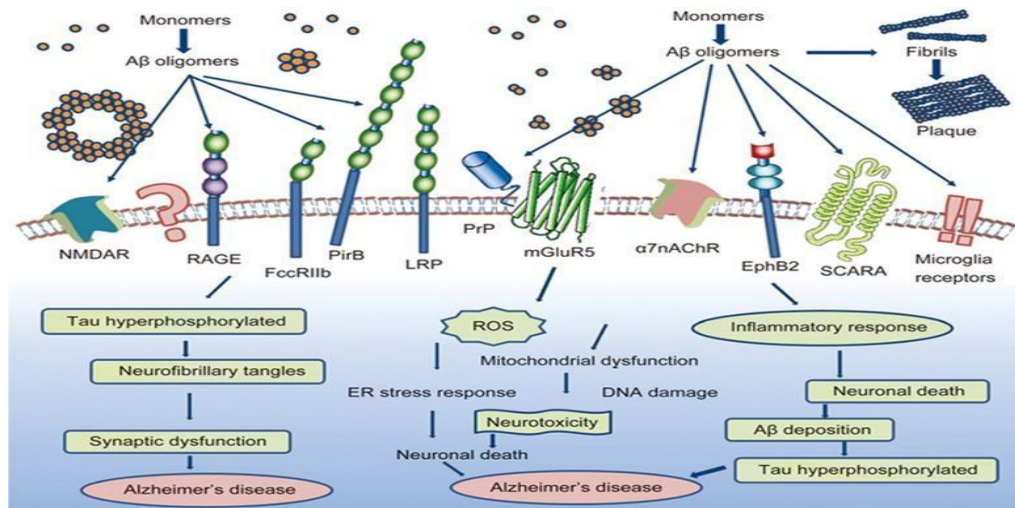
Figure.1 Amyloid hypothesis [2]

APP belongs to the class of glycoproteins and has a crucial function in various essential activities, such as neuronal development and signaling, intracellular transport, and other aspects of neuronal homeostasis [3]. Aβ peptides are 37-42 amino acid residues derived from the proteolytic cleavage of APP and are characterized by their definitive hairpin bend. Between the two proteolysis pathways of APP, Aβ is produced through the Amyloidogenic pathway (Figure2) in which the Amyloid Precursor Protein is cleaved by β-secretase to give the membrane-tethered C-terminal fragments β (CTFβ or C99) and N-terminal sAPPβ. Then, cleavage of C99 by γ-secretase takes place to produce extracellular Aβ monomers [3], [4].
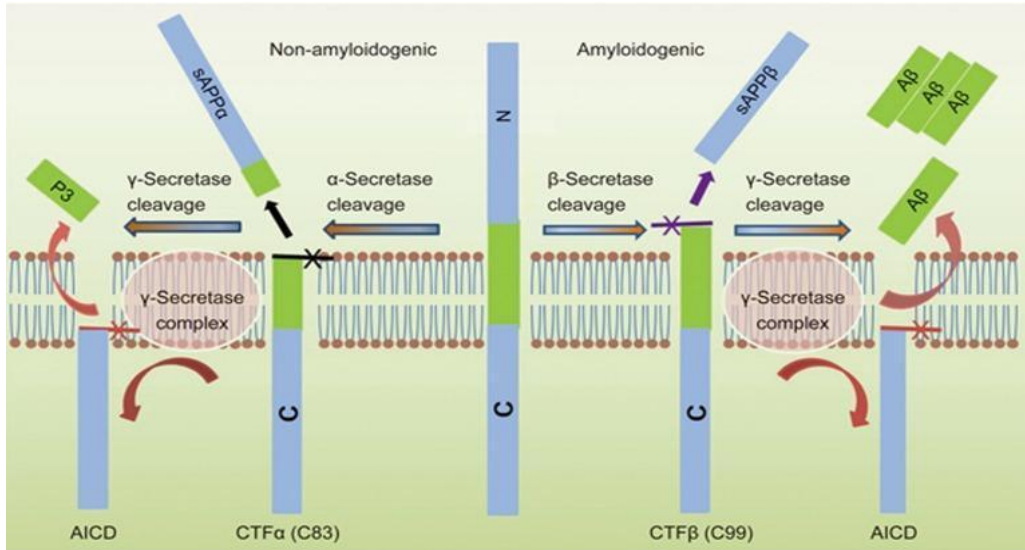
Figure.2 Proteolytic pathway of APP [3]

While a standard amount (small and unknown) of Amyloid-beta is essential for memory and associated functions, an excessive amount of Amyloid-beta peptide, in turn, aggregates to form insoluble oligomers, which in turn form plaques that settle between neurons and eventually interrupt the communication between them and are neurotoxic at the same time. Further, these Aβ oligomers interrupt the functioning of various receptors and enzymes, which causes a complete dysfunction in neuronal cells.

6.3 Role of selenium in AD

Selenium (Se) is an element that was regarded to be toxic till the 1950s. The discovery of twenty-five Selenoproteins that play a significant role in several critical metabolic processes and pathways has changed that notion, and Se under a standard amount is extremely important to the human body, with several studies showing the benefits of a selenium-rich diet. It is also shown that in several places, the intake of Se is far lower than the required dietary range.

A nine-year longitudinal study in France has shown that over time, the probability of cognitive impairment increases with a decline in plasma Se, although the same study has reported no association between short-term alteration (2 years) of Se and change in cognitive function [5], [6].

High mortality rates are frequently observed in elderly people with low Se [7]. A secondary cross-sectional analysis of data from a study has shown that meals including fish are correlated with Se uptake as well. Similarly, a secondary analysis of a 10-year prospective cohort study showed that people who consume supplemental antioxidants, including Se and zinc, are associated with a 34% reduced risk of developing cognitive impairment when compared to people who do not consume antioxidants [8], [9].

Several studies have shown that the brains of AD patients have low levels of Se content and that long-term consistent intake of Se supplementation might help in reducing the intensity of AD [9]. These studies show that the inclusion of Se in drugs proves to be beneficial with enhanced biological activity.

6.4 Thiosemicarbazones

Thiosemicarbazones are ligands that have showcased their ability to exhibit a wide range of biological activities, including anti-cancer, anti-tumor, and anti-inflammatory properties, and a few TSC ligands have reached clinical trials as anti-cancer and anti-tumor drugs, exhibiting significant activity. The presence of multiple donor atoms in TSCs and their ability to undergo tautomerism and metal chelating effect plays a significant part in the above. While these ligands have been studied extensively for various diseases, the information about their activity in AD is limited.

Thione form   Thiol form
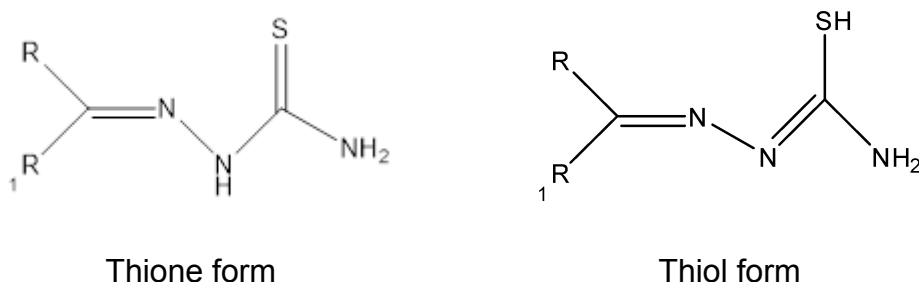
Figure 3. Tautomerization forms of TSCs

The few TSCs that have been studied for AD have shown significant activity as Amyloid-beta inhibitors and have exhibited good cytotoxic activity, which might be attributed to their planar core structure and coordination ability [10]. These ligands also afford a great advantage, as the thiosemicarbazone backbone can act as a bridge

13

appending any two scaffolds of our choice. The TSC moiety exhibits excellent hydrogen bonding ability with Aβ and further helps in assisting the interaction between the Aβ peptide and our aromatic scaffold [11].
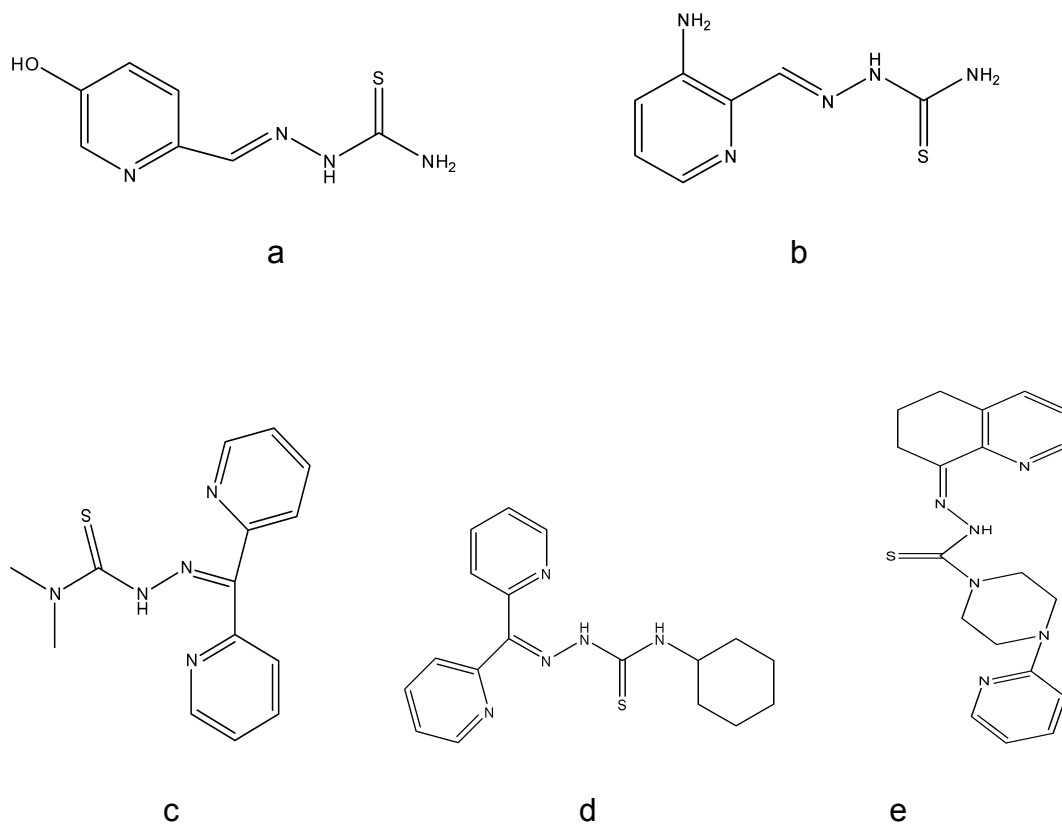
Figure 4. TSCs in clinical trials

a	2-formyl-5-hydroxypyridine TSC	Anti-Cancer
b	Triapine	Anti-Cancer
c	Dp44mT	Anti-tumor
d	DpT	Anti-Cancer
e	COTI	Anti-Cancer

Table 1. TSCs in clinical trials

6.5 Acyl-Selenoureas

Selenoureas are a class of compounds that are commonly used as precursors for the introduction of selenium into heterocycle compounds. At the same time, selenoureas, as ligands themselves, exhibit extensive biological activity and are studied for various pharmacological purposes. Similar to thiosemicarbazones, selenoureas have not been studied much for AD and amyloid inhibition. The published selenourea derivatives have shown good biological activity and are tunable with fragments of our choice.

Selenoureas show excellent free radical scavenging properties [12], enzyme inhibition activity, anticancer activity [13], GPx-like activity [14], and DNA binding properties and are much more efficient than their sulfur counterparts [15], [16] in these fields. This encourages us to synthesize selenoureas and compare their activity to their corresponding thioureas in terms of amyloid inhibition and associated toxicity.

The aim of this project is to synthesize thiosemicarbazone derivatives and acyl-selenourea derivatives as inhibitors of Aβ aggregation and associated toxicity.

7. Materials and methods

7.1 Experimental

All chemical compounds and solvents used in this project were directly purchased from commercial sources and used without any modifications. A Bruker 400 MHz spectrometer was used to record ^{1}H, ^{13}C, and ^{77}Se spectras. $CDCl_3$ and DMSO-d_6 were used as solvents to record the spectra with TMS as the internal standard. The Solvent signals are (δH= 7.26ppm, δC= 77.2ppm) for CDCl3 and (δH= 0.00, δC= 0.0) for internal TMS. Chemical shifts (δ) in the spectras are presented in parts per million, and coupling constants (J) are presented in Hertz. Nicolet-iS5 spectrophotometer was used to record FT-IR spectras in the form of KBr pellets. Shimadzu-2600 spectrophotometer was used to record UV-Vis spectras with DMF as the solvent. All the reactions were monitored to completion using TLC under UV light.

7.2 Computational

Vega-ZZ was used for the conformational search of the ligands, and Gaussian09W along with Gaussview was used for the DFT studies. GOLD and HERMES from the CCDC package were used for Molecular docking, while the SwissADME webserver was used for calculating the ADMET properties of the compounds.

8. Synthesis and characterization

8.1 Synthesis of thiosemicarbazones (TSCs):

All the thiosemicarbazone ligands were synthesized by following the general method, and the extraction methods differ according to the description below them.

To an ethanolic solution of 4-methyl thiosemicarbazide/ 4-phenyl thiosemicarbazide (1 mmol in 10 mL), an equivalent amount of the corresponding ketone (1 mmol) in ethanol (10 mL) was added with continuous stirring. A catalytic amount of Glacial acetic acid was added, and this mixture was refluxed at 65-68°C for 24-40 hrs.
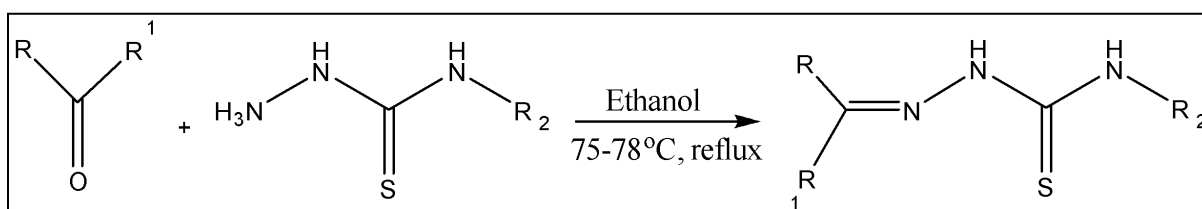
Scheme 1. Synthesis of Thiosemicarbazones

8.1.1 (E)-2-(chroman-4-ylidene)-N-methylhydrazine-1-carbothioamide

1
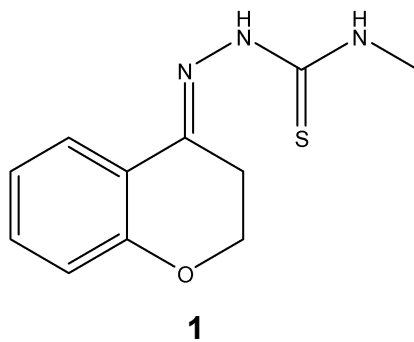
After completion of the reaction as monitored by TLC, the mixture was cooled to room temperature. The obtained product was washed with cold EtOH and recrystallized in acetonitrile to afford pure white crystal needles.

Yield= 92%; ^{1}H NMR (500 MHz, CDCl$_3$) δ 8.69 (s, 1H), 7.86 (dd, J = 8.0, 1.7 Hz, 1H), 7.57 (s, 1H), 6.91 (ddd, J = 8.2, 7.3, 1.2 Hz, 1H), 6.84 (dd, J = 8.3, 1.2 Hz, 1H), 4.22 (t, J = 6.2 Hz, 2H), 3.21 (d, J = 4.9 Hz, 3H), 2.70 (t, J = 6.2 Hz, 2H). ^{13}C NMR (500 MHz, CDCl$_3$) δ 178.53, 157.58, 141.42, 131.63, 124.39, 121.70, 119.69, 117.93, 64.48, 31.36, 25.14.

8.1.2 (E)-2-(chroman-4-ylidene)-N-phenylhydrazine-1-carbothioamide
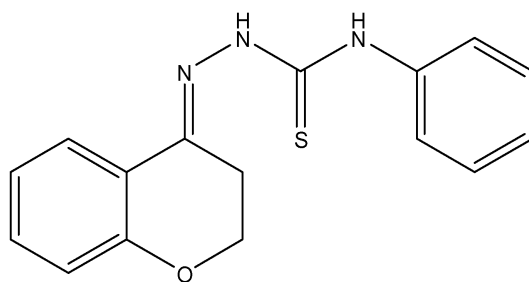
2

The same extraction method as compound **1** was used. White crystalline needles were obtained from crystallization in acetonitrile.

Yield= 86%; ^{1}H NMR (500 MHz, DMSO-d$_6$) δ 9.83 (s, 1H), 9.00 (s, 1H), 8.90 (d, J=4.9 Hz, 2H), 8.50 (s, 2H), 8.43 (s, 1H), 8.19 (m, 2H), 7.79 (s, 1H), 7.28 (dd, J=7.2, 2.1 Hz, 1H), 4.06 (s, 2H), 3.52 (s, 2H). ^{13}C NMR (500 MHz, DMSO-d$_6$) δ 162.96, 154.66, 146.66, 144.69, 143.23, 143.16, 140.41, 126.99, 126.91, 124.04, 120.56, 118.73, 117.53, 117.34, 115.96, 112.64.

8.1.3

(Z)-2-((E)-3-(3-chlorophenyl)-1-phenylallylidene)-N-methylhydrazine-1-carbothioamide
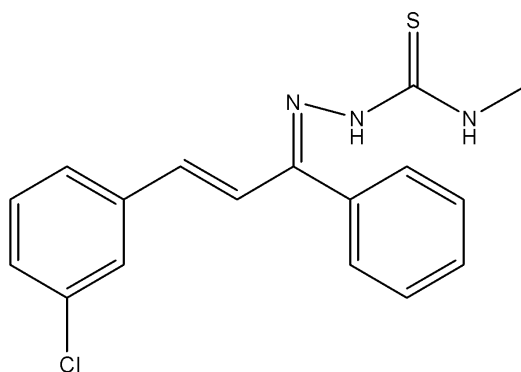
3

After completion of the reaction as monitored by TLC, the solvent was evaporated under reduced pressure to obtain the crude brownish yellow colored residue. Then hexane was added to the mixture to wash off the impurities. Acetonitrile was added and the

obtained yellow organic layer was filtered. Yellow crystals were obtained upon slow evaporation of the organic layer.

Yield=71%; ^{1}H NMR (500 MHz, DMSO-d$_6$) δ 9.72 (s, 1H), 9.46 (d, J=4.7 Hz, 1H), 9.14 (s, 1H), 8.62 (m, 2H), 8.20 (m, 2H), 7.81 (s, 1H), 4.34 (d, *J* = 7.1 Hz, 3H), 3.89 (s, 1H), 3.25 (t, *J* = 4.5 Hz, 2H), 2.52 (t, *J* = 5.4 Hz, 3H). ^{13}C NMR (500 MHz, DMSO-d$_6$) δ 164.49, 152.64, 151.90, 149.02, 147.16, 147.99, 146.81, 146.49, 119.52, 119.28, 118.75, 117.76, 115.64, 112.59, 56.00, 34.76, 21.11.

8.1.4

(Z)-2-((E)-3-(3-chlorophenyl)-1-phenylallylidene)-N-phenylhydrazine-1-carbothioamide
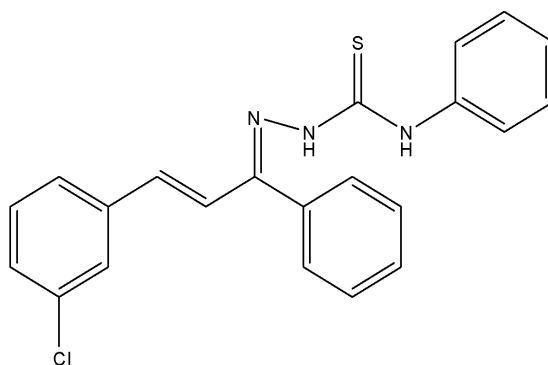
4

After completion of the reaction as monitored by TLC, cold H$_2$O was added to the reaction mixture. The mixture was filtered, and the obtained brown precipitate was purified by recrystallization in EtOH.

Yield=83%; ^{1}H NMR (500 MHz, DMSO-d$_6$) δ 10.59 (s, 1H), 8.56 (q, *J* = 4.7 Hz, 1H), 8.29 (s, 1H), 8.22 (td, *J* = 7.8, 1.8 Hz, 3H), 7.48 – 7.42 (m, 2H), 7.29 – 7.22 (m, 2H), 7.03 (d, *J* = 4.6 Hz, 3H), 6.29 (m, 1H), 6.21 (m, 1H), 3.04 (s, 1H), 2.73 (s, 1H). ^{13}C NMR (500 MHz, DMSO-d$_6$) δ 172.70, 163.51, 143.36, 138.11, 136.46, 136.34, 135.78, 134.30, 133.83, 133.24, 132.95, 129.60, 129.26, 129.24, 128.84, 128.69, 128.67, 128.51, 128.10, 122.55, 42.31, 30.80.

8.1.5 (E)-2-(4H-chromen-4-ylidene)-N-methylhydrazine-1-carbothioamide
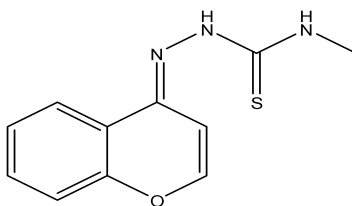
5

After completion of the reaction as monitored by TLC, the majority of solvent was evaporated under reduced pressure. MDC: Hexane (1: 1) was added to the remaining mixture, and the obtained precipitate was recrystallized from EtOH.

Yield=%; Brown; ^{1}H NMR (500 MHz, DMSO-d$_6$) δ 9.89 (s, 1H), 9.22 (s, 1H), 8.28 (t, J = 1.8 Hz, 1H), 8.12 (s, 1H), 7.79 (dt, J = 7.8, 1.2 Hz, 1H), 7.59 (ddd, J = 8.1, 2.1, 1.0 Hz, 1H), 7.55 – 7.51 (m, 2H), 3.26 (s, 3H). ^{13}C NMR (500 MHz, DMSO-d$_6$) δ 172.88, 154.65, 144.12, 141.14, 139.26, 135.82, 132.68, 130.15, 128.41, 128.07, 31.04.

8.1.6 (E)-2-(4H-chromen-4-ylidene)-N-phenylhydrazine-1-carbothioamide
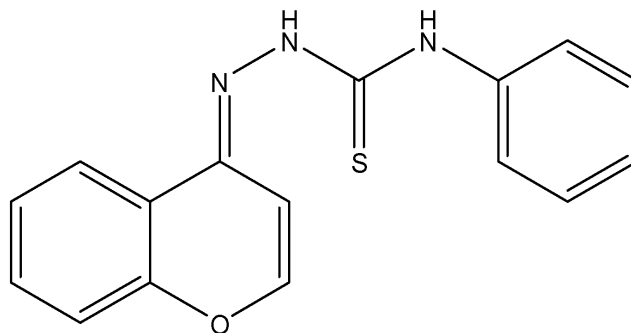
6

The same extraction method as compound **5** was used. The compound was recrystallized from acetonitrile.

Yield=%; Brown; ^{1}H NMR (500 MHz, DMSO-d$_6$) δ 10.50 (s, 1H), 10.46 (s, 1H), 9.14 (s, 1H), 8.62 (s, 1H), 8.20 (m, 2H), 7.81 (s, 1H), 7.52 (m, 2H), 7.46 (d, J=4.7 Hz, 1H), 7.41 (m, 2H), 7.26 (s, 1H). ^{13}C NMR (500 MHz, DMSO-d$_6$) δ 170.89, 162.44, 148.99, 147.12, 147.00, 143.98, 130.50, 130.16, 130.05, 128.48, 128.41, 126.88, 125.38, 125.20, 124.28, 122.33.

8.2. Synthesis of selenoureas:

All the selenourea ligands were synthesized using the following general procedure.

Theonyl chloride/ Furanyl chloride (1 mmol) in dry acetone (10 mL) was added to a solution of Potassium selenocyanate (1 mmol) in dry acetone (10 mL) with continuous stirring. The reaction was allowed to run at RT for 1 hr. To the obtained intermediate yellow precipitate (isothiocyanate), an equivalent amount of the corresponding amine (1 mmol) in dry acetone (10 mL) was added with continuous stirring. This reaction was allowed to run at RT for 24-30 hrs. After the completion of the reaction as monitored by TLC, the reaction mixture was added to 150 mL of 1N HCl. After some time, the resulting precipitate was filtered and washed several times with H_2O.
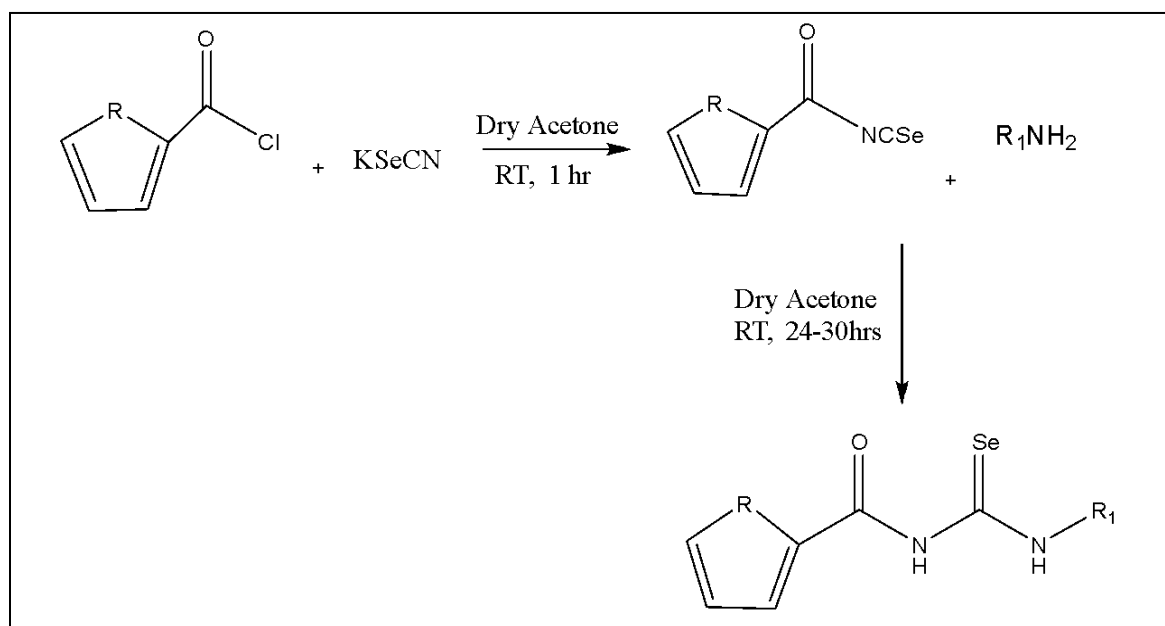
Scheme 2. Synthesis of Acyl-selenoureas

8.2.1 N-(phenylcarbamoselenoyl)furan-2-carboxamide
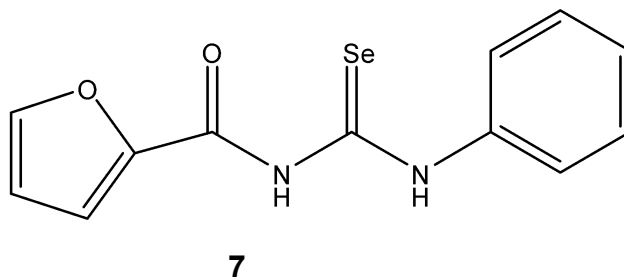
7

Yield=27%; Red; ^{1}H NMR (500 MHz, CDCl$_3$) δ 12.69 (s, 1H), 8.54 (s, 1H), 7.86 (dd, J = 8.0, 1.7 Hz, 1H), 7.57 (s, 1H), 6.91 (ddd, J = 8.2, 7.3, 1.2 Hz, 1H), 6.84 (dd, J = 8.3, 1.2 Hz, 1H), 6.70 (t, J = 6.2 Hz, 2H), 6.21 (d, J = 4.9 Hz, 1H), 6.07 (t, J = 6.2 Hz, 1H). ^{13}C NMR (500 MHz, CDCl$_3$) δ 178.53, 157.58, 145.72, 143.29, 141.42, 131.63, 124.39, 121.70, 119.69, 117.93.

8.2.2 N-((4-nitrophenyl)carbamoselenoyl)furan-2-carboxamide
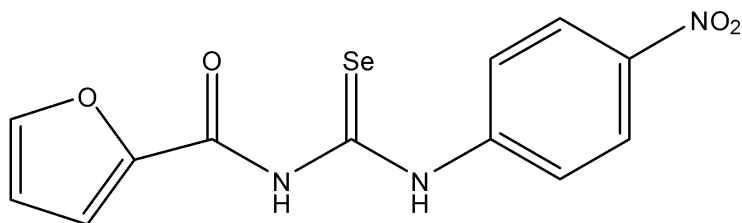
8

Yield= 36%; ^{1}H NMR (400 MHz, CDCl$_3$) δ 13.12 (s, 1H), 9.55 (s, 1H), 8.23 (dd, J = 9.6, 2.7 Hz, 2H), 8.00 (dd, J = 9.5, 2.7 Hz, 2H), 7.62 (d, J = 1.8 Hz, 1H), 7.39 (d, J = 3.7 Hz, 1H), 6.62 (dd, J = 3.7, 1.7 Hz, 1H). ^{13}C NMR (400 MHz, CDCl$_3$) δ 179.93, 156.71, 147.10, 144.31, 125.23, 124.64, 124.03, 120.05, 119.22, 113.80, 113.10. 77Se NMR (400 MHz, CDCl3) δ 482.39.

8.2.3 N-(pyrazine-2-ylcarbamoselenoyl)furan-2-carboxamide
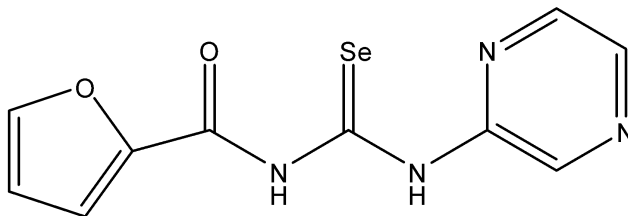
9

Yield= 54% ;Red; ^{1}H NMR (500 MHz, DMSO) δ 11.93 (s, 1H), 9.00 (s, 1H), 8.90 (s, 1H), 8.50 (m, 2H), 8.19 (s, 1H), 7.79 (d, J=4.7Hz, 2H). ^{13}C NMR (500 MHz, DMSO) δ 169.96, 154.66, 146.66, 140.41, 126.99, 124.04, 120.56, 117.53, 115.96, 112.64.

8.2.4 N-(phenylcarbamoselenoyl)thiophene-2-carboxamide
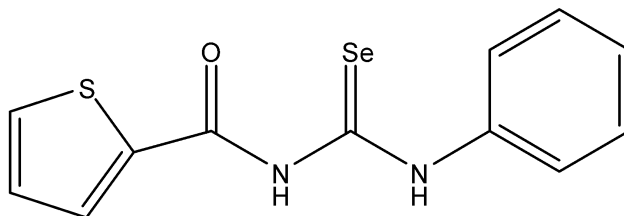
10

Yield= 48% ; Slimy green; ^{1}H NMR (500 MHz, DMSO) δ 12.89 (s, 1H), 10.22 (s, 1H), 8.28 (t, *J* = 1.8 Hz, 1H), 8.12 (s, 1H), 7.79 (dt, *J* = 7.8, 1.2 Hz, 1H), 7.59 (ddd, *J* = 8.1, 2.1, 1.0 Hz, 1H), 7.55 – 7.51 (m, 2H), 7.38 (td, *J* = 7.8, 2.4 Hz, 1H), 7.25 – 7.21 (m, 1H). ^{13}C NMR (500 MHz, DMSO) δ 172.88, 154.65, 144.12, 141.14, 138.07, 135.82, 132.68, 130.15, 128.41, 128.07.

8.2.5 N-((4-nitrophenyl)carbamoselenoyl)thiophene-2-carboxamide
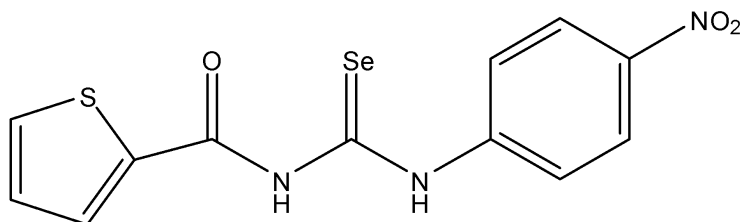
11

Yield= 32%; Pastel orange; ^{1}H NMR (500 MHz, DMSO) δ 11.89 (s, 1H), 10.22 (s, 1H), 8.28 (t, *J* = 1.8 Hz, 1H), 8.12 (s, 1H), 7.79 (dt, *J* = 7.8, 1.2 Hz, 1H), 7.59 (ddd, *J* = 8.1, 2.1, 1.0 Hz, 1H), 7.55 – 7.51 (m, 2H). ^{13}C NMR (500 MHz, DMSO) δ 173.68, 154.65, 144.25, 143.69, 141.14, 138.11, 136.49, 135.82, 132.68, 130.15, 128.41, 126 03.

8.2.6 N-(pyrazin-2-ylcarbamoselenoyl)thiophene-2-carboxamide
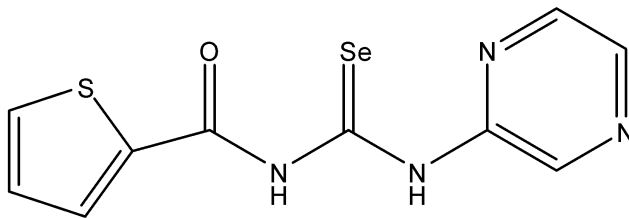
12

Yield=26.09%; Brown; ^{1}H NMR (500 MHz, DMSO) δ 11.67 (s, 1H), 10.83 (s, 1H), 8.85 (s, 1H), 8.37 (s, 1H), 7.53 (dt, *J* = 7.4, 1.7 Hz, 1H), 7.59 (m, 1H), 7.51 (m, 2H). ^{13}C NMR (500 MHz, DMSO) δ 169.88, 157.27, 148.67, 145.67, 140.43, 133.16, 132.13, 129.85, 129.00, 118.01.

8.3 NMR spectra

Representative NMR spectra for compounds **1** (TSC) and **8** (Selenourea)
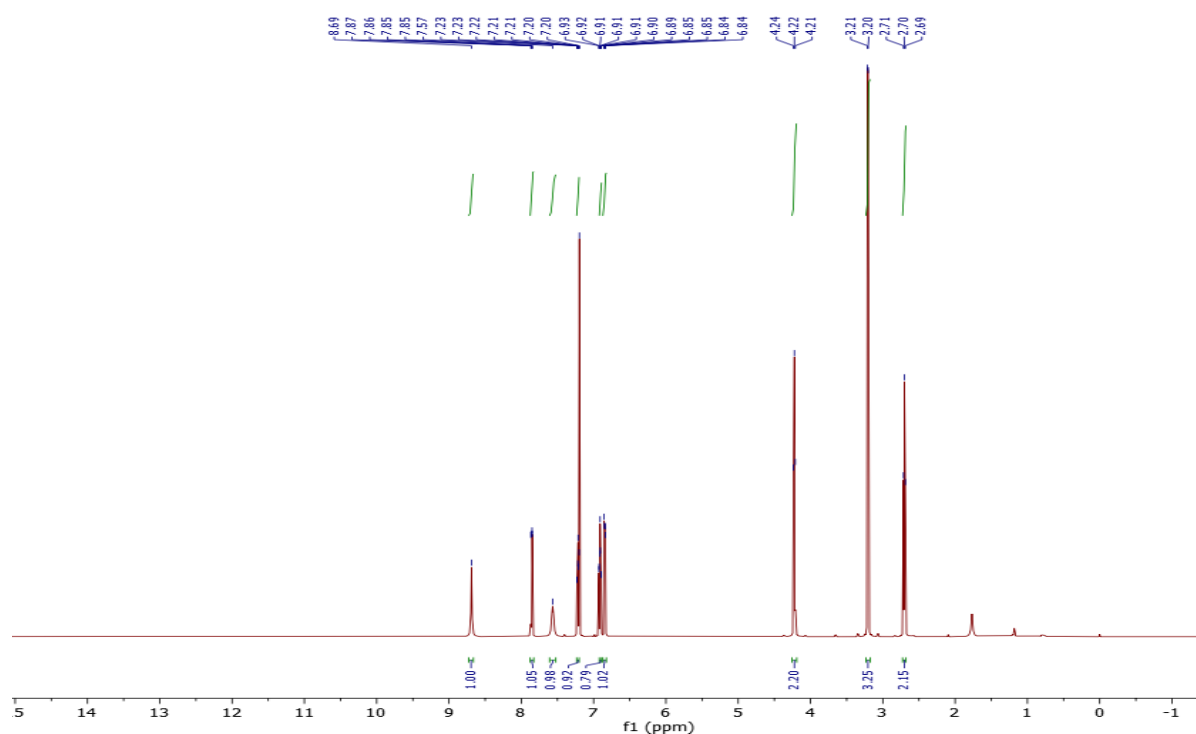
Figure 5.1 ^{1}H NMR of compound **1**
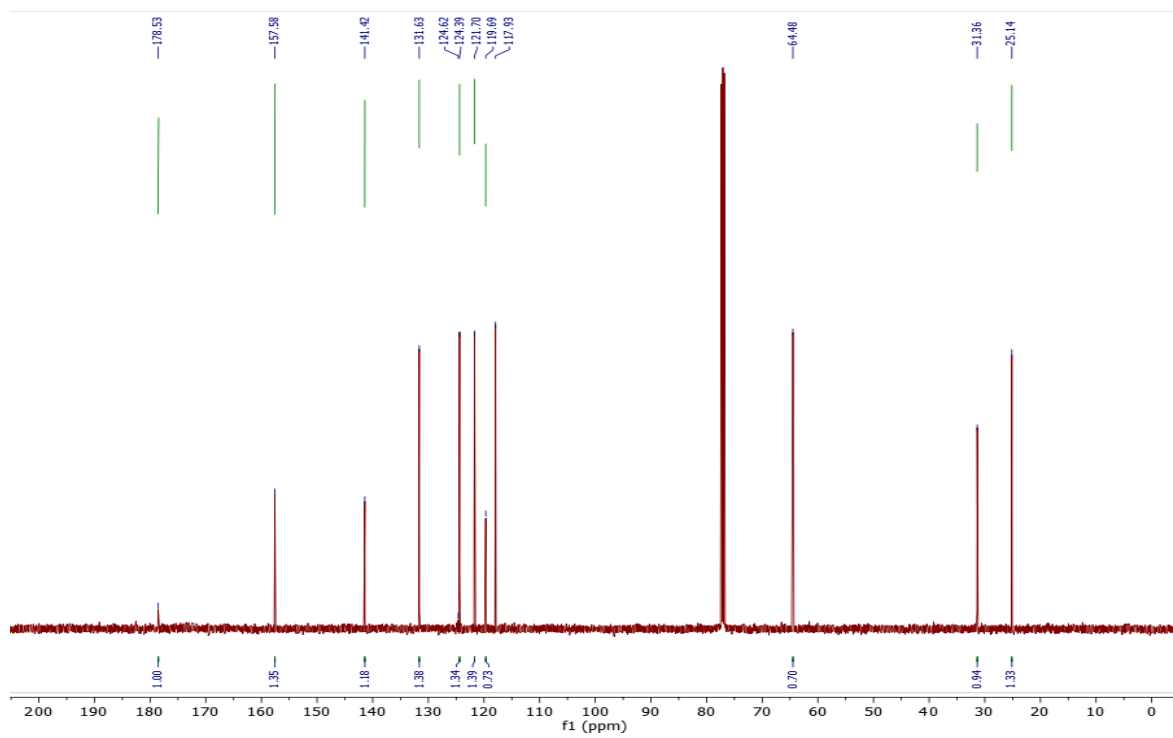
Figure 5.2 ^{13}C NMR of compound **1**
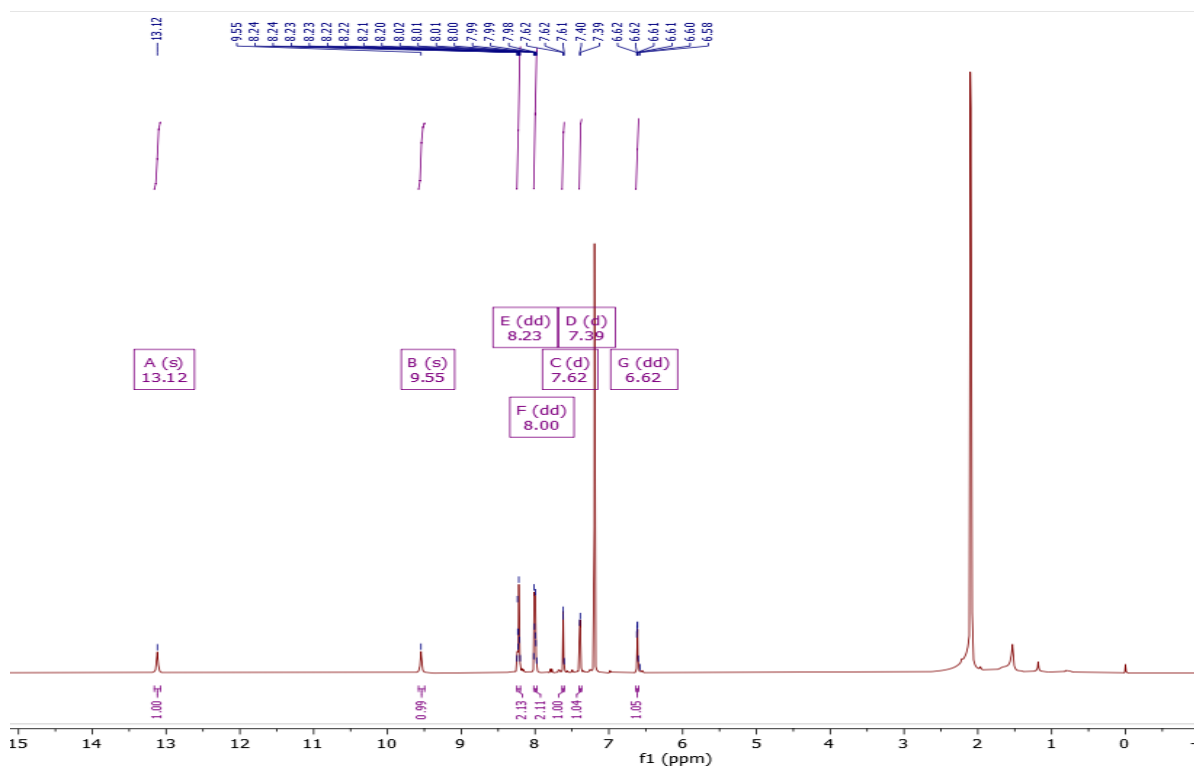
Figure 6.1 ^{1}H NMR of compound **8**
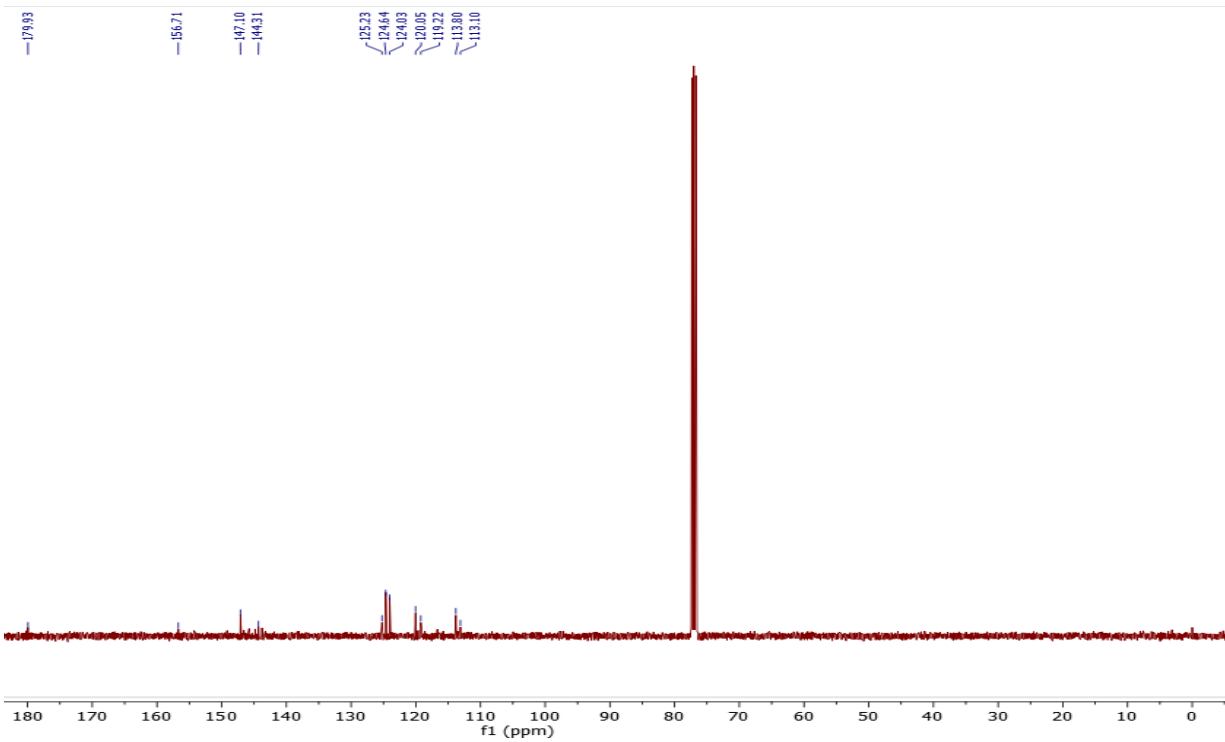
Figure 6.2 ^{13}C NMR of compound **8**
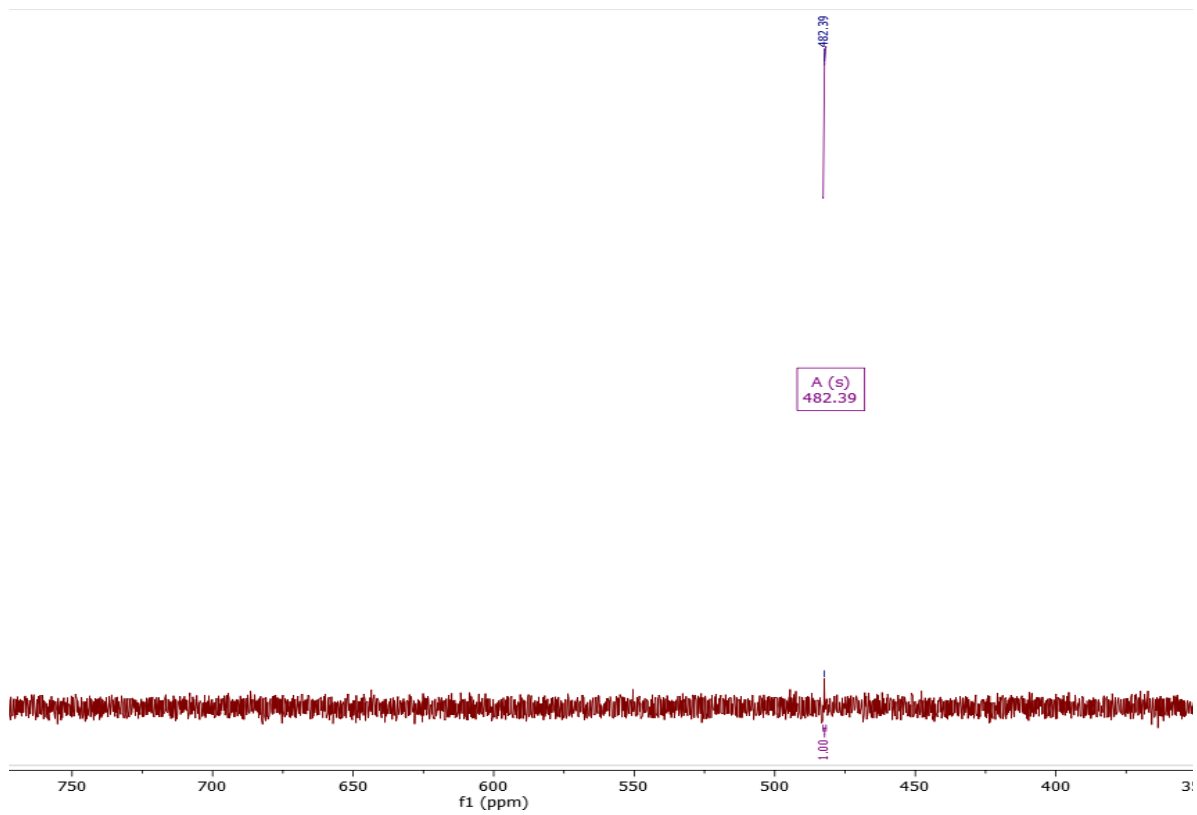
Figure 6.3 ^{77}Se NMR of compound

9. Computational studies

9.1 Conformational search

Vega-ZZ was used for performing a conformational search of all the ligands. SMILES code was used to build the 3D structures, to which atomic potential was assigned using the CHARMM protocol, and Gasteiger charges were assigned to all the atoms. All the flexible torsions were taken into account with 10 rotation steps, and systematic search parameters were used. The Toler condition was set to 0.01 under the conjugate gradients method. The protocol was completed when the Toler condition was true or the number of steps was reached.

9.2 DFT studies

The final structure from the conformational search was used as the input structure for further computation since Gaussian uses a single-point search algorithm. Gaussian 09W was invoked through Gaussview, and geometry optimization was performed for all the ligands. The basis sets were decided through a literature search, and the sets which enabled the closest value to the experimental crystal structures were used.

All the ligands underwent geometry optimization through the DFT method using a hybrid functional B3YLP. The LANL2DZ basis set was preferred for Thiosemicarbazones, while the 6311G++(d,p) basis set was preferred for the Acyl-selenoureas [17]. The opt+freq option was used to check for convergence along with the optimization.

9.3 Molecular docking

Protein Data Bank was used as the source for obtaining all the protein structures used in the study (PDB id: 1iyt, 2lfm, 2beg). The GOLD software for docking was invoked using HERMES, which is also used for protein preparation and visualization. All the water and ligand molecules were removed, hydrogens were added, and the protonation state was set. In this case, blind docking was performed since the size of the proteins are small (40-42 amino acids), and there are multiple sites for binding.

Since GOLD does not allow blind docking, the whole protein was set as the binding site.

The optimized ligands from the DFT studies were directly used for docking using the genetic algorithm. ChemScore was the scoring function used, and they were rescored using CHEMPLP. The docking conformations with high Chemscore, PLP fitness, Hydrogen bonding ability, and favorable distances were picked. The results were then visualized and analyzed through HERMES and Discovery studio.

9.4 ADMET properties

The SwissADME web server was used for determining "ADMET(absorption, distribution, metabolism, excretion, and toxicity) drug-like properties of all the ligands concerning Lipinski's rule of 5" [18]. SwissADME calculates a molecule's bioavailability, lipophilicity, pharmacokinetics, physicochemical properties, and hence the drug-likeliness using the 2-D structure of a molecule.

10. Results and discussion

10.1 DFT studies

10.1.2 MEP analysis

1 **3**

8 **9**
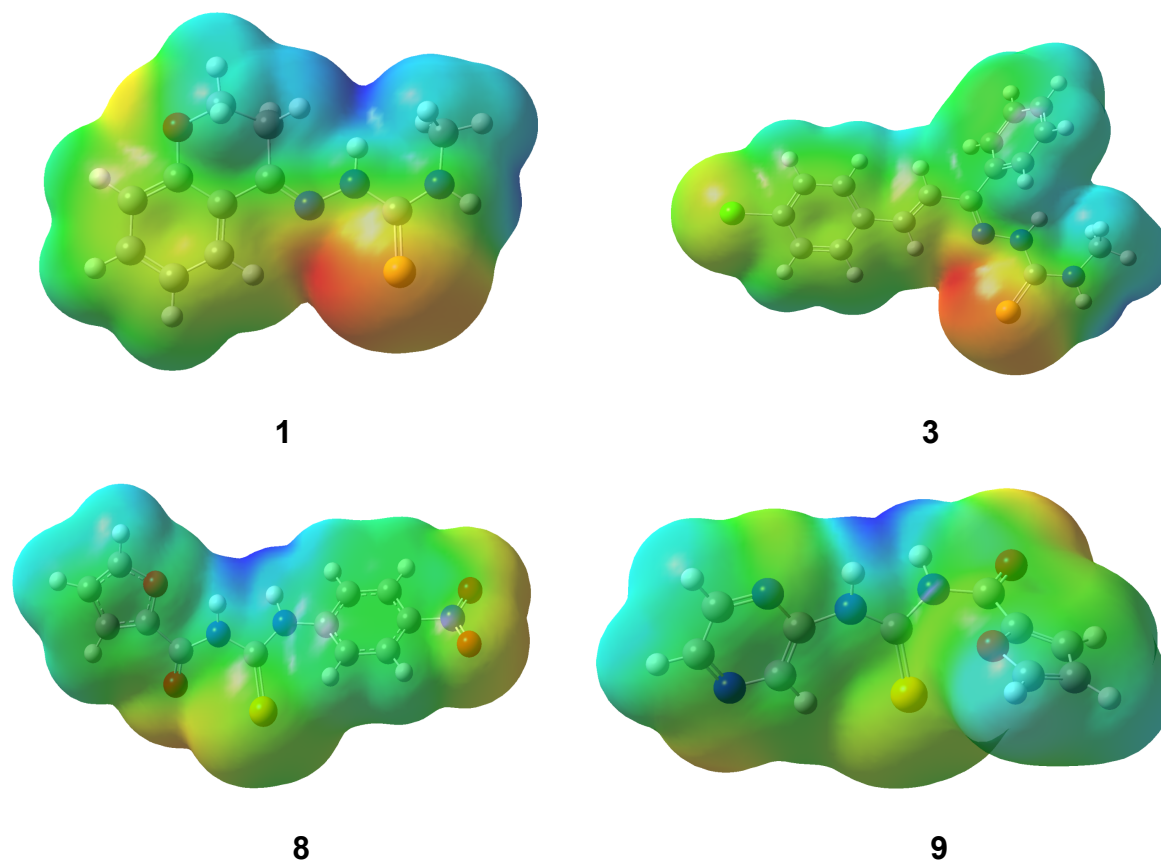
Figure 7 Representative ESP structures of TSCs (**1,3**) and acyl-selenoureas (**8,9**).

All the 3D ESP maps are built within a fixed range of charges, and the areas with the highest electronegativity are represented in red, while the areas with lower electronegativity are represented in blue.

The ESP surface diagrams reveal that the electron density is highest on the sulfurs in the thiosemicarbazones along with the oxygen in the benzopyran moiety in compounds **1, 2, 5, 6**, and chlorine in compounds **3, 4**. In the selenoureas, the electron density is

observed to be highest on the carbonyl oxygen and the nitro group in compounds **8,** and **11,** followed by selenium in all the compounds.

10.1.3 Frontier molecular analysis
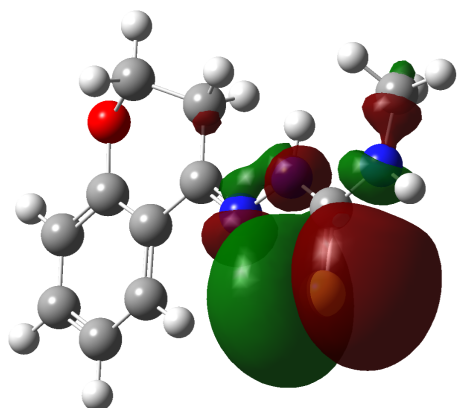
HOMO	LUMO
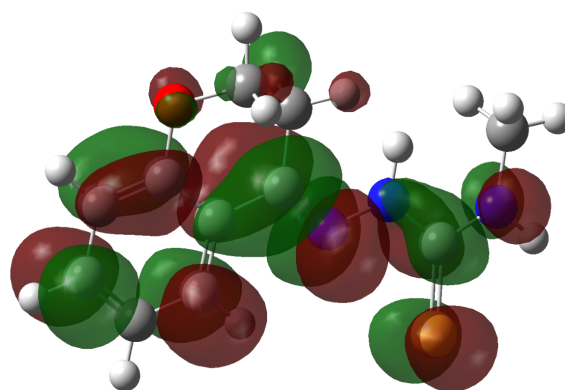
1
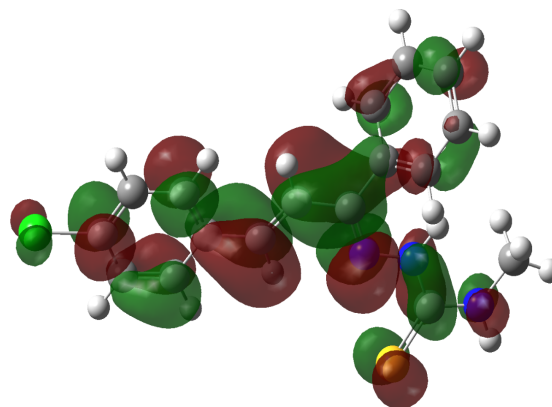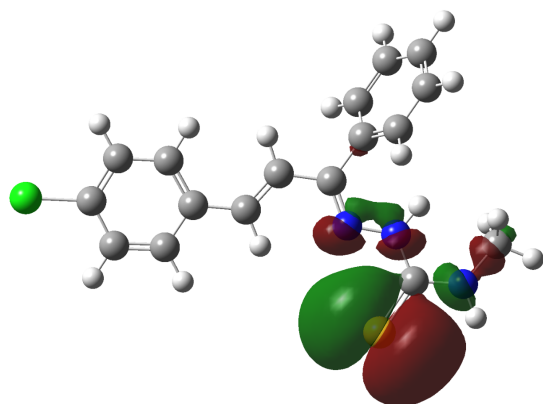
3
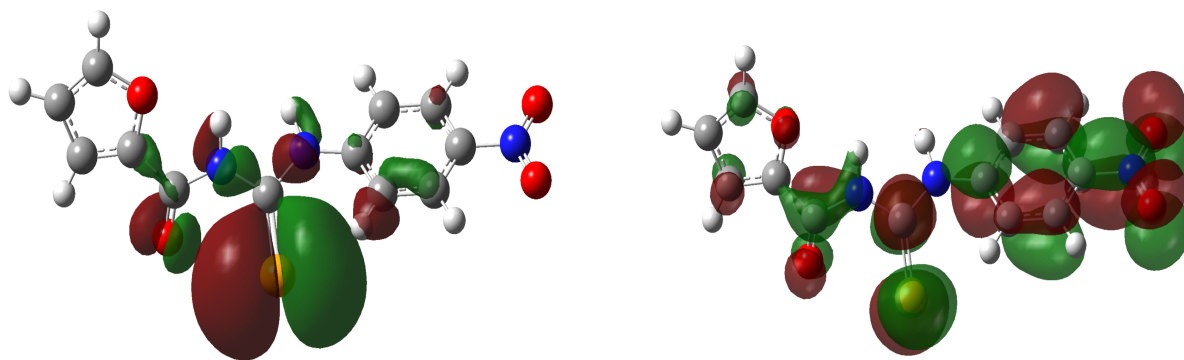
8
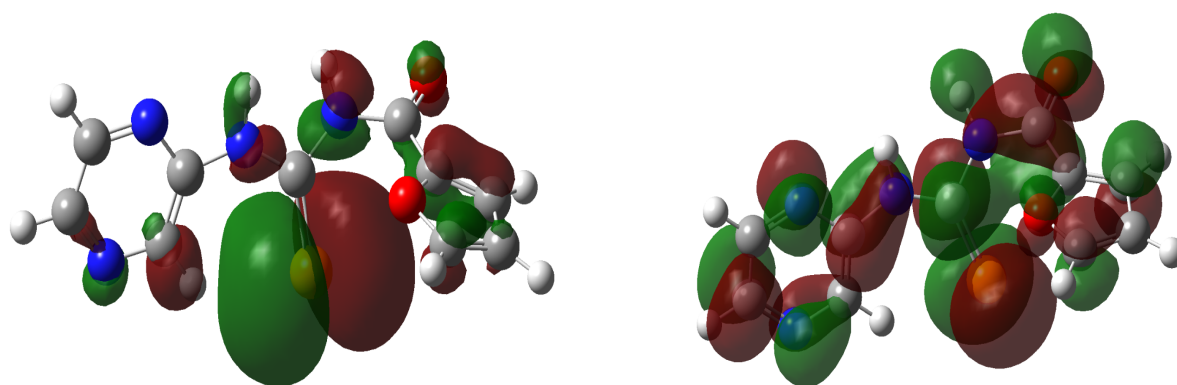
9

Figure 8 Representative HOMO-LUMO structures of TSCs (**1,3**)

and acyl-selenoureas (**8,9**).

In compounds **1-6,** the formation of HOMOs mainly occurs in the *p*-orbitals of sulfur, whereas the LUMOs are observed on the chromone and chalcone rings. In compounds **7-12**, the HOMOs are formed by the selenium orbitals, while the LUMOs are seen on the furan/ thiophene rings. The HOMO-LUMO energy gaps, which provide information regarding chemical stability, have been calculated for all the compounds and are tabulated along with their dipole moments in **Table 2**.

	HOMO(eV)	LUMO(eV)	HOMO-LUMO (eV)	Energy (a.u.)	Dipole moment (Debye)
1	-0.19508	-0.05879	0.13629	-676.438008	7.143693
2	-0.20786	-0.06943	0.13843	-868.153218	4.247548
3	-0.19376	-0.08068	0.11308	-846.567855	9.167208
4	-0.20057	-0.08316	0.11741	-1038.277943	8.607726
5	-0.19033	-0.06498	0.12535	-675.221680	6.766069
6	-0.20150	-0.07412	0.12738	-866.937085	5.566076
7	-0.19928	-0.07920	0.12008	-3124.975760	6.709123
8	-0.21805	-0.11081	0.10724	-3329.539315	9.453194
9	-0.22137	-0.09129	0.13008	-3157.058700	3.522432
10	-0.21417	-0.09268	0.09268	-3447.980318	4.264484
11	-0.21311	-0.11065	0.10246	-3652.506774	9.359411
12	-0.20651	-0.09603	0.11048	-3480.052490	6.679517

Table 2 DFT optimized parameters of the compounds.

Dipole moment is directly related to the stability of a molecule. Lower the dipole moment, the higher the stability. The TSCs containing phenyl substituent instead of methyl show more stability. There is no observable difference between the HOMO-LUMO energy gaps between the molecules.

10.2 Molecular docking

The most common interactions observed in the docked structures are H-bonding, Vanderwaal's, pi-alkyl interactions, pi-pi T-shaped interactions, and salt bridges. The amyloid monomer protein structures follow their characteristic hairpin bend starting from the N-terminal to their GLY25 residue with the 1st bend in the middle (around GLU11) and the 2nd bend from the GLY25 residue to the end C-terminal. All the docked compounds (both TSCs and acyl-selenoureas) are enclosed within the 1st bend and interact with the amino acid residues within this bend as seen in the residues involved.

The amyloid pentamer protein displays parallel stacking of the monomers and forms a single but broader bend in their structures.

Higher Chemscore means higher binding ability, and high PLP fitness means higher rescore, which in turn means the probability of the accuracy of the predicted pose is high.

10.2.1 Interactions with Aβ_{40} monomer

	Interactions	H-bonding	Chemscore/ PLP
1	GLU3, PHE4, ARG5, GLY9, TYR10, GLU11, VAL12, HIS13, LYS16, VAL18, GLU22	GLN15	18.5720
			36.8399
2	PHE4, ARG5, SER8, GLY9, GLU11, VAL12, HIS13, LYS16, VAL18, PHE19, GLU22	GLN15, TYR10	22.0935
			35.2846
3	ASP1, ALA2, PHE4, ARG5, ASP7, GLN15, VAL18, GLU22, VAL24	GLU3	25.5359
			47.4097
4	ASP1, ALA2, GLU3, PHE4, ARG5, ASP7, SER8, VAL12, HIS13, HIS14, LYS16, VAL12, GLN15, VAL18, GLU22, VAL24		28.8928
			58.8084
5	ASP1, ALA2, GLU3, PHE4, ARG5, ASP7, SER8, VAL12, HIS13, HIS14, GLN15, LYS16, VAL18, GLU22, VAL24		21.3353
			27.8898
6	ASP1, GLU3, PHE4, HIS6, ASP7, SER8, GLY9, GLN15, VAL18, ALA21, GLU22, VAL24	ARG5	23.6355
			46.3051

Table 3 Compounds 1-6 with Aβ_{40} monomer

3   **6**
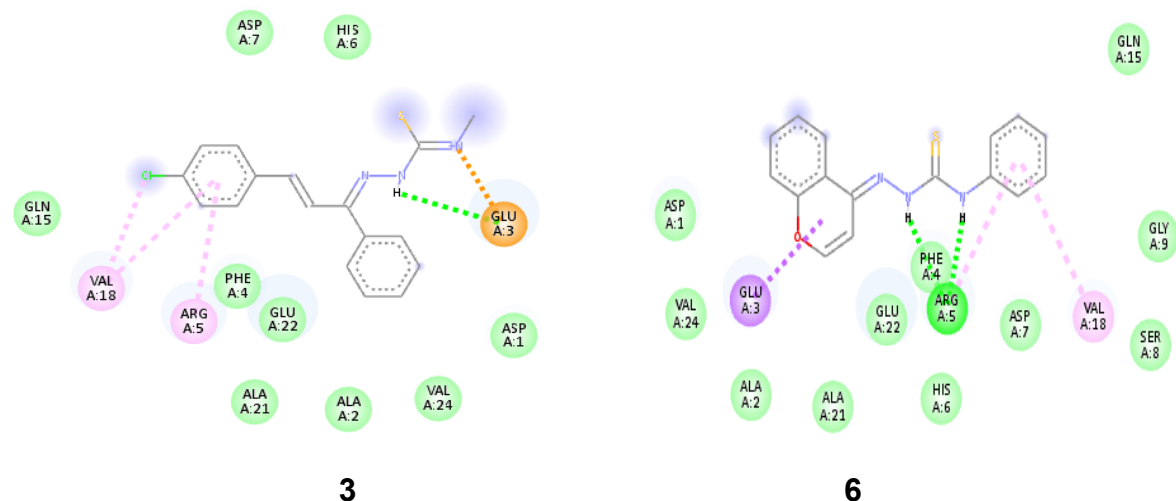
Figure 9

Compounds 3 and 4 show the best binding poses and pi-alkyl interactions in residues ARG5 and VAL18 are the most commonly observed interactions among all the compounds. Similarly, residues PHE4, GLN15, and GLU22 are involved in bonding in all the compounds.

	Interactions	H-bonding	Chemscore/ PLP
7	GLY9, GLU11, HIS13, LYS16, VAL18	SER8, TYR10, GLN15	21.9866
			39.8644
8	PHE4, ARG5, HIS6, GLY9, TYR10, VAL18	SER8, ASP7, GLN15	21.8172
			41.2519
9	GLY9, GLU11, VAL12, HIS13, LYS16	SER8, TYR10, GLN15	18.0527
			24.2358
10	GLY9, GLU11, HIS13, LYS16, VAL18, GLU22	SER8, TYR10, GLN15	19.3388
			32.1178
11	PHE4, ARG5, HIS6, GLY9, TYR10, VAL18	ASP7, SER8, GLN15	21.4329
			40.8912
12	ALA2, GLU3, PHE4, ARG5	GLU22	17.8045
			25.0868

Table 4 Compounds 7-12 with $A\beta_{40}$ monomer

8 **11**
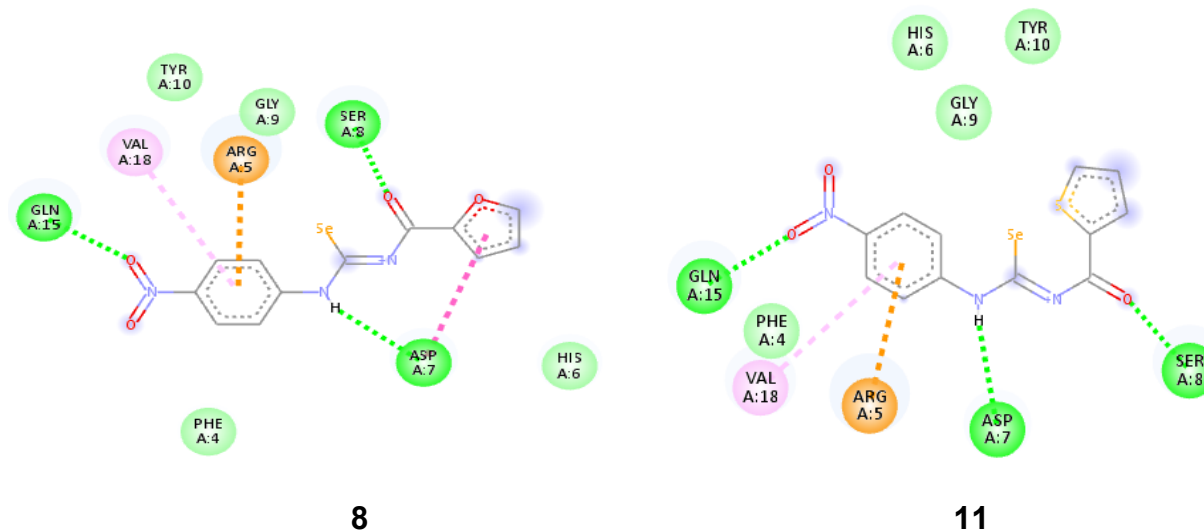
Figure 10

SER8, TRY10, and GLN15 are the amino acids responsible for forming H-bonding interactions in acyl-selenoureas with the $A\beta_{40}$ monomer. All the structures except compound **12** exhibit H-bonding (C=O) with SER8 residue. Compound **8** shows the best binding ability among all the acyl-selenourea compounds.

10.2.2 Interactions with $A\beta_{42}$ monomer

	Interactions	H-bonding	Chemscore/ PLP
1	VAL12, GLN15, PHE19, PHE20	LYS16	19.1479
			30.5132
2	VAL12, GLN15, PHE19, PHE20	LYS16	22.0218
			33.0309
3	VAL12, LYS16, VAL18, PHE19, GLU22	GLN15	23.9471
			32.6140
4	VAL12, HIS13, GLN15, PHE19, PHE20, ASP23	LYS16	27.1091
			44.2072
5	SER8, GLY9, GLU11, VAL12, LYS16,	GLN15	18.0320

	PHE19		31.2916
6	VAL12, GLN15, PHE19, PHE20, ASP23	LYS16	21.6532
			36.1882

Table 5 Compounds 1-6 with $A\beta_{42}$ monomer

3 **4**
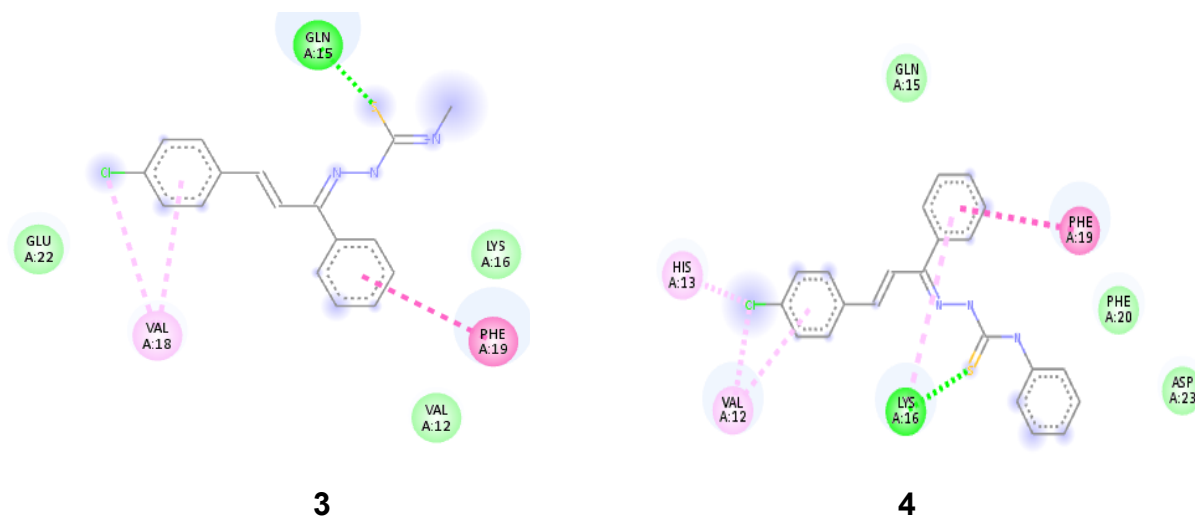
Figure 11

LYS 16 and GLN15 are the main amino acids responsible for H-bond interactions with sulfur in the bonding of TSC compounds to the amyloid-beta monomer(1-42). Compounds **3** and **4** show the best binding ability among all the compounds. The residues VAL12, PHE19, and PHE20 are also involved in bonding in all the compounds.

	Interactions	H-bonding	Chemscore/ PLP
7	VAL12, GLN15, PHE19, PHE20	LYS16	17.7208
			28.8476
8	SER8, GLU11, VAL12, LYS16, PHE19, PHE20	ASP7, GLN15	21.4214
			47.3268
9	ASP7, SER8, GLU11, VAL12, LYS16, PHE19	GLN15	17.1884
			25.4022
10	VAL12, GLN15, PHE19, PHE20	LYS16	18.6544
			31.0006

11	ASP7, SER8, GLU11, VAL12, PHE19, PHE20	GLN15, LYS16	20.5505
			35.5393
12	VAL12, PHE19, PHE20, ASP23	GLN15, LYS16	19.0864
			37.3258

Table 6 Compounds 7-12 with Aβ_{42} monomer

8   **11**
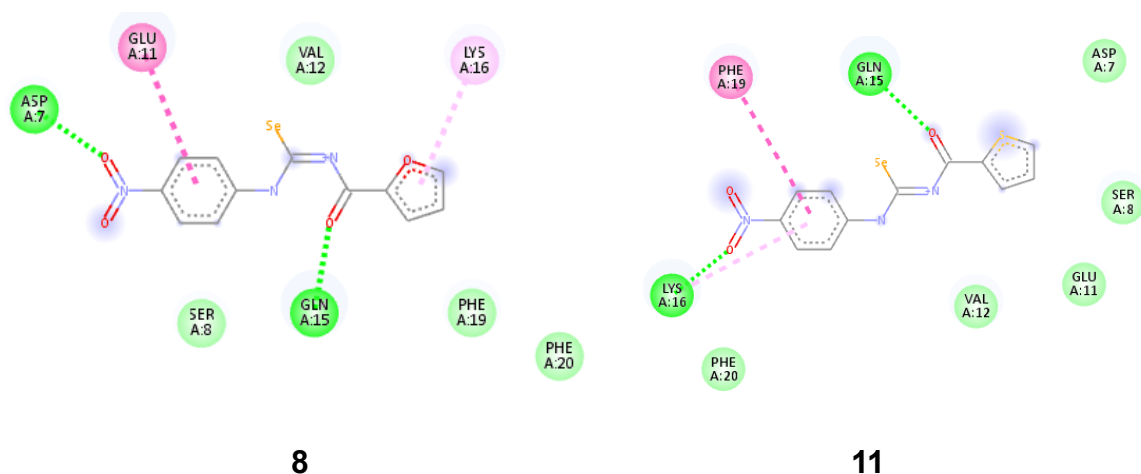
Figure 12

GLN15 and LYS16 are responsible for H-bonding with both the NH protons. Vanderwaal's interactions in VAL12, PHE19, and PHE20 residues are present in all the structures. Compound **8** shows the best interactions among all the compounds.

10.2.3 Interactions with Aβ-pentamer

	Interactions	H-bonding	Chemscore/ PLP
1	LEU17, VAL18, PHE20, GLY37, GLY38, VAL39, VAL40	PHE19	19.7146
			34.4592
2	LEU17, VAL18, PHE20, GLY37, GLY38, VAL39, VAL40	PHE19	23.2882
			36.8388
3	PHE19, ALA21, GLU22, ASP23, LEU34, VAL36, GLY37, GLY38		24.5658
			38.2483
4	PHE19, ALA21, GLU22, ASP23,	ALA21	24.9403

	LEU34, VAL36, GLY38		43.1256
5	PHE19, PHE20, ALA21, GLU22, ASP23, LEU34, VAL36	PHE19, ALA21	20.7347
			34.8405
6	PHE20, ALA21, GLU22, VAL36, GLY37, GLY38, VAL39, VAL40	PHE19	23.0299
			46.3647

Table 7 Compounds 1-6 with Aβ-pentamer

2   **4**
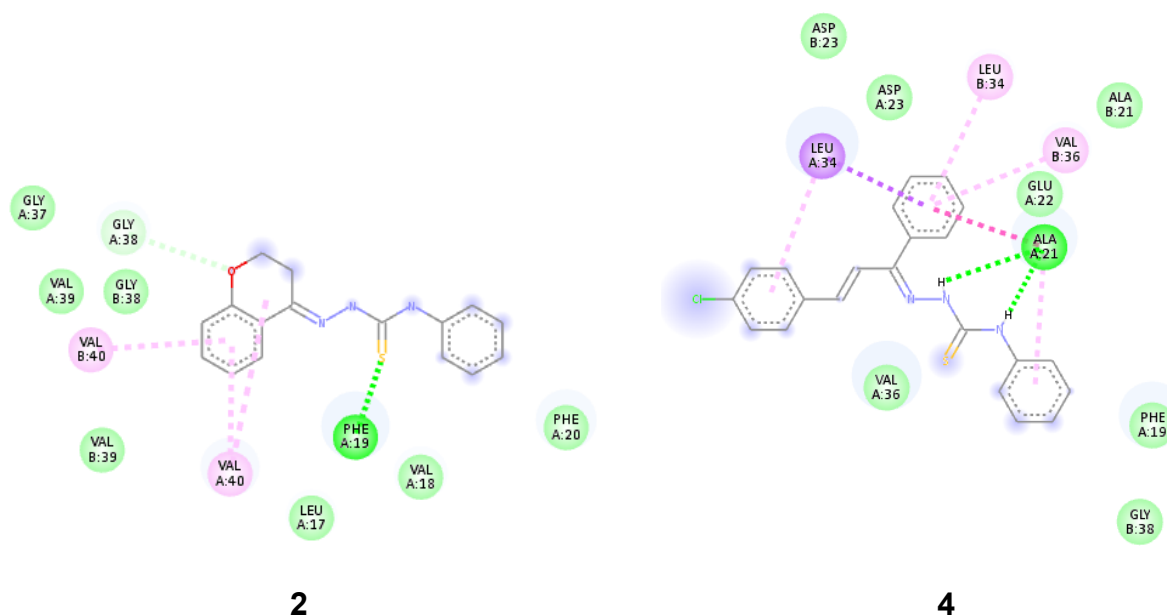
Figure 13

PHE19 and ALA21 are the most common amino acid residues responsible for forming H-bonding with the compounds by either interacting with the sulfur or both the NH residues in the TSCs. Compounds **3** and **4** show the best binding interactions among all the compounds. GLY38 is also involved in exhibiting Vanderwaal's interactions with all the compounds.

	Interactions	H-bonding	Chemscore/ PLP
7	PHE19, PHE20, GLU22, ASP23, LEU34, VAL36, GLY37, GLY38, VAL39, VAL40	ALA21	21.9008
			37.3184
8	PHE20, GLU22, VAL36, GLY37, GLY38	PHE19, ALA21	21.6638

			45.9379
9	PHE19, PHE20, GLU22, VAL36, GLY37, GLY38	ALA21	19.2999
			32.0583
10	PHE20, GLU22, VAL36, GLY37, GLY38, VAL39, VAL40	PHE19, ALA21	23.5166
			49.1023
11	PHE20, ALA21, GLU22, VAL36, GLY37, GLY38	PHE19	21.6874
			45.5858
12	LEU17, VAL18, PHE20, ALA21, GLU22	PHE19	21.4549
			48.8218

Table 8 Compounds 7-12 with Aβ-pentamer

8   **10**
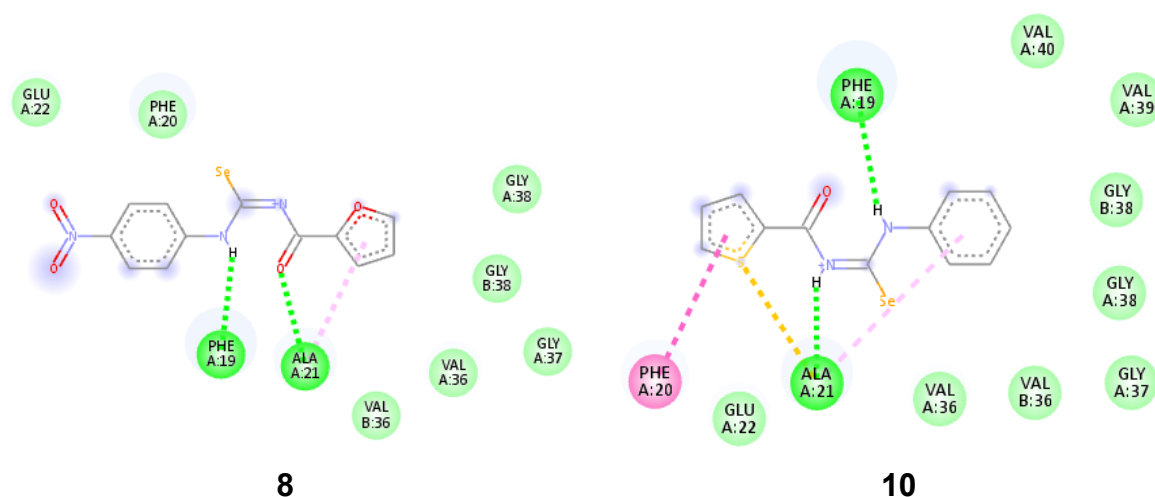
Figure 14

Similar to TSCs, PHE19 and ALA21 are the residues responsible for H-bonding between the amyloid-beta pentamer protein and the acyl-selenourea compounds. Residues PHE20 and GLU22 are also involved in Vanderwaal's interaction with all the compounds making the four residues involved a hotspot for binding.

10.3 ADMET properties

	1	2	3	4	5	6
PHYSICOCHEMICAL PROPERTIES						
Formula	C11H13N3OS	C16H15N3OS	C17H16ClN3S	C22H18ClN3S	C11H11N3OS	C16H13N3OS
Molecular weight (g/mol)	235.31	297.37	329.85	391.92	233.29	295.36
Heavy atoms	16	21	22	27	16	21
Aromatic heavy atoms	6	12	12	18	10	16
Fraction Csp^3	0.27	0.12	0.06	0.00	0.09	0.00
Rotatable bonds	3	4	6	7	3	4
H-bond acceptors	2	2	1	1	2	2
H-bond donors	2	2	2	2	2	2
Molar Refractivity	67.29	88.50	97.53	118.75	65.84	87.06
TPSA [$Å^2$]	77.74	77.74	68.51	68.51	81.65	81.65
Consensus Log $P_{o/w}$	1.75	3.09	3.13	3.13	1.85	3.13
PHARMACOKINETICS						
GI absorption	high	high	high	high	high	high
BBB permeant	no	yes	no	no	no	no
P-gp	no	no	no	no	no	no

substrate						
CYP1A2 inhibitor	yes	yes	yes	yes	yew	yes
CYP2C19 inhibitor	no	yes	yes	yes	yes	yes
CYP2C9 inhibitor	no	yes	yes	yes	no	yes
CYP2D6 inhibitor	no	yes	yes	yes	no	yes
CYP3A4 inhibitor	no	yes	yes	yes	no	yes
Log Kp (skin permeation) [cm/s]	-6.61 cm/s	-5.88 cm/s	-5.74 cm/s	-5.74 cm/s	-6.74 cm/s	-5.74 cm/s
DRUGLIKENESS						
Lipinski	yes	yes	yes	yes	yes	yes
Ghose	yes	yes	yes	yes	yes	yes
Veber	yes	yes	yes	yes	yes	yes
Egan	yes	yes	yes	yes	yes	yes
Muegge	yes	yes	yes	yes	yes	yes
Bioavailability Score	0.55	0.55	0.55	0.55	0.55	0.55
MEDICINAL CHEMISTRY						
PAINS	0 alert	0 alert	0 alert	0 alert	0 alert	0 alert
Leadlikeness	no	yes	yes	yes	no	yes
Synthetic accessibility	2.86	3.07	3.44	3.44	3.35	3.44

Table 9. ADMET properties of compounds 1-6.

	7	8	9	10	11	12
PHYSICOCHEMICAL PROPERTIES						
Formula	C12H10 N2O2Se	C12H9N 3O4Se	C10H8N 4O2Se	C12H10 N2OSSe	C12H9N 3O3SSe	C10H8N 4OSSe
Molecular weight (g/mol)	293.18	338.19	295.16	309.25	354.24	311.22
Heavy atoms	17	20	17	17	20	17
Aromatic heavy atoms	11	11	11	11	11	11
Fraction Csp^3	0.00	0.00	0.00	0.00	0.00	0.00
Rotatable bonds	5	6	5	5	6	5
H-bond acceptors	2	4	4	1	3	3
H-bond donors	2	2	2	2	2	2
Molar refractivity	66.48	75.31	62.07	72.10	80.92	67.69
TPSA [Å^2]	54.27	100.09	80.05	69.37	115.19	95.15
Consensus Log P$_{o/w}$	0.97	0.45	-0.21	1.60	1.08	0.42
PHARMACOKINETICS						
GI absorption	high	high	high	high	high	high
BBB permeant	yes	no	no	yes	no	no
P-gp substrate	no	no	no	no	no	no
CYP1A2 inhibitor	no	no	no	no	no	no
CYP2C19	no	no	no	no	no	no

inhibitor						
CYP2C9 inhibitor	no	no	no	no	no	no
CYP2D6 inhibitor	no	no	no	no	no	no
CYP3A4 inhibitor	no	no	no	no	no	no
Log Kp (skin permeation) (cm/s)	-6.48	-6.88	-7.77	-6.14	-6.54	-7.44
DRUGLIKENESS						
Lipinski	yes	yes	yes	yes	yes	yes
Ghose	yes	yes	yes	yes	yes	yes
Veber	yes	yes	yes	yes	yes	yes
Egan	yes	yes	yes	yes	yes	yes
Muegge	yes	yes	yes	yes	yes	yes
Bioavailability score	0.55	0.55	0.55	0.55	0.55	0.55
MEDICINAL CHEMISTRY						
PAINS	0 alert	0 alert	0 alert	0 alert	0 alert	0 alert
Leadlikeness	yes	yes	yes	yes	no	yes
Synthetic accessibilty	2.46	2.62	2.86	2.34	2.51	2.76

Table 10. ADMET properties of compounds 7-12.

The tabulated ADMET properties show that all the synthesized compounds obey all 5 rules for predicting drug-likeness. They also exhibit high GI-absorption index and bioavailability score. Only 3 of the 12 compounds exhibit BBB permeability properties.

BBB permeability is an important factor in transporting drugs to the brain, which is essential for Alzheimer's. While this is a huge problem, we can try lipid-mediated transport of the drugs as an alternative.

The synthesized compounds were also docked with AChE, BuChEand 5-HT receptors. The docking results show good binding ability with all the receptors. So, our compounds do not exhibit any selectivity towards the Amyloid-beta peptide.

11. Conclusion

We have synthesized six thiosemicarbazone and six acyl-selenourea ligands and characterized them through NMR, IR, and UV and have computationally studied their activity against Amyloid-beta aggregation. We have also identified the primary amino acid residues which are responsible for interacting with the Amyloid-beta peptides. .

This study can be further extended with the inclusion of selenium in the TSCs for an increase in activity to anti-aggregation properties. The molecular dynamic studies of the protein-ligand interactions might be able to present a clearer picture of the mechanism for these interactions.

Low selectivity of the compounds is an issue due to which the compounds cannot be used directly as amyloid-beta inhibitors, but these compounds can be used as lead compounds for further optimization.

12. References

[1] "Alzheimer's disease is a type of brain disease". 2022 Alzheimer's disease facts and figures. *Alzheimer's. Dement*. **2022**, 18, 700-789.

[2] Hardy, J.; Selkde, D. J. The amyloid hypothesis of alzheimer's disease: Progress and problems on the road to therapeutics. *Science.* **2002**, 297, 353-356.

[3] Chen, G. F.; Yan, Y.; Zhou, Y. R.; Jiang, Y.; Melcher, K.; Xu, H. E. Amyloid beta: structure, biology and structure-based therapeutic development. *Acta. Pharmacologica. Sinica.* **2017**, 38, 1205-1235.

[4] Barrow, C. J.; Small, D. H. Abeta peptide and alzheimer's disease. *Springer. London*. **2007,** 1, 1-37.

[5] Akbaraly, T. N.; Hininger-Favier, I.; Carriere, I.; Arnaud, J.; Gourlet, V.; Roussel A. M.; Berr, C. Plasma selenium over time and cognitive decline in the elderly. *Epidemiology.* **2007**, 18, 52-58.

[6] Berr, C.; Arnaud, J.; Akbaraly, N. T. Selenium and cognitive impairment: A brief-review based on results from the EVA study. *Biofactors*. **2012**, 38, 139-144.

[7] Akbaraly, N. T.; Arnaud, J.; Hininger-Favier, I.; Gourlet, V.; Roussel, A. M.; Berr, C. Selenium and mortality in the elderly: results from the EVA study. *Clin. Chem.* **2005**, 51, 2117-2123.

[8] Gray, S. L.; Hanlon, J. T.; Landerman, L. R.; Artz, M.; Schmader, K. E.; Fillenbaum, G. G. Is antioxidant use protective of cognitive function in the community-dwelling elderly? *Am. J. Geriatr. Pharmacother.* **2003**, 1, 3-10.

[9] Loef, M.; Schrauzer, G. N.; Walach, H. Selenium and alzheimer's disease: A systematic review. *Journal. of. Alzheimer's. Disease.* **2011**, 26, 81-104.

[10] Sagnou, M.; Mavroidi, B.; Kaminari, A.; Boukos, N.; Pelecanou, M. Novel isatin thiosemicarbazone derivatives as potent inhibitors of β-amyloid peptide aggregation and toxicity. *ACS. Chem.* **2020**, 11, 2266-2276.

[11] Ranade, D. S.; Shravage, B. V.; Kumbhar, A. A.; Sonawane, U. B.; Jani, V. P.; Joshi, R. R.; Kulkarni, P. P. Thiosemicarbazone moiety assist in interaction of planar aromatic molecules with amyloid beta peptide and acetylcholinesterase. *Chemistry. Select.* **2017**, 2, 3911-3916.

[12] Merino-Montiel, P.; Maza, S.; Martos, S.; López, O.; Maya, I.; Fernández-Bolaños, J. G. Synthesis and antioxidant activity of O-alkyl selenocarbamates, selenoureas and selenohydantoins. *Eur. J. Pharm. Sci.* **2013**, 48, 582-592.

[13] Tsukagoshi, H.; Koketsu, M.; Kato, M.; Kurabayashi, M.; Nishina, A.; Kimura, H. Superoxide radical-scavenging effects from polymorphonuclear leukocytes and toxicity in human cell lines of newly synthesized organic selenium compounds. *The. FEBS. Journal.* **2007**, 274, 6046-6054.

[14] Roldán-Peña, J. M.; Alejandre-Ramos, D.; López, O.; Maya, I.; Lagunes, I.; Padrón, J. M.; Peña-Altamira, L. E.; Bartolini, M.; Monti, B.; Bolognesi, M. L.; Fernandez-Bolaños, J.G. New tacrine dimers with antioxidant linkers as dual drugs: Anti-Alzheimer's and antiproliferative agents. *Eur. J. Med. Chem.* **2017**, 138, 761-773.

[15] Yiğit, M.; Celepci, D. B.; Taslimi, P.; Yiğit, B.; Çetinkaya, E.; Özdemir, I.; Aygün, M.; Gülçin, I. Selenourea and thiourea derivatives of chiral and achiral enetetramines: Synthesis, characterization and enzyme inhibitory properties. *Bioorganic Chemistry.* **2022,** 120, 105566.

[16] Reddy, M. V. B.; Srinivasulu, D.; Peddanna, K.; Apparao C. H.; Ramesh, P. Synthesis and antioxidant activity of new thiazole analogues possessing urea, thiourea, and selenourea functionality. *Synthetic. Communications.* **2015**, 45, 2592-2600.

[17] Vyas, N. A.; Singh, S. B.; Kumbhar, A.S.; Ranade, D.S.; Walke, G.R.; Kulkarni, P. P.; Jani, V.; Sonavane, U. B.; Joshi, R. R.; Rapole, S. Acetylcholinerase and Aβ aggregation inhibition by heterometallic ruthenium(II)-platinum(II) polypyridyl complexes. *Inorg. Chem*. **2018**, 57, 7524-7535.

[18] Daina, A.; Michielin, O.; Zoete, V. SwissADME: a free web tool to evaluate pharmacokinetics, drug-likeness and medicinal chemistry friendliness of small molecules. *Sci. Rep*. **2017**, 7.